acta physica slovaca vol. 55 No. 3, 315 – 322 **June 2005**

INTERFERENCE MULTILAYER MIRRORS FOR X-RAY AND EXTREME ULTRAVIOLET OPTICS[1]

M. Jergel[a,1,2], M. Ožvold[a,b], R. Senderák[a], E. Majková[a], Š. Luby[a]

[a] *Institute of Physics, Slovak Academy of Sciences, Dúbravská cesta 9, 845 11 Bratislava, Slovakia*

[b] *Department of Materials Engineering, Faculty of Materials Science and Technology, Slovak University of Technology, J.Bottu 24, 917 24 Trnava, Slovakia*

Received 11 February 2005, accepted 23 February 2005

Ultrashort period (1.5–3.2 nm) Cu/Si and Ni/C multilayers for X-ray interference mirrors are presented. The multilayers were prepared by ultra-high vacuum electron beam deposition onto a heated substrate. An optimum deposition temperature of 80°C was found in both cases. The multilayer quality was probed by the specular X-ray reflectivity and interface diffuse scattering at $CuK_{\alpha 1}$ wavelength. An asymmetry between the metal-on-metalloid and metalloid-on-metal interfaces was detected, the larger interface width amounting to 0.5 nm and 0.65 nm in Cu/Si and Ni/C, respectively. It is induced mainly by the metal layer growth and diffusion of metalloid into metal. Thermal stability tests were performed. Cu/Si mirrors are applicable only at operation temperatures below 100°C while the Ni/C multilayer breakdown occurred at 350°C. Ni/C mirrors are superior to Cu/Si ones also in terms of shorter vertical and lateral correlation lengths with important implications for the specular imaging contrast.

PACS: 41.50.+h, 42.25.Fx, 61.10.Kw, 68.65.Ac

1 Introduction

Interference multilayer mirrors have become an indispensable part of instrumentation in astronomy, lithography, plasma diagnostics, at synchrotron storage rings and in other fields. They are composed of regularly alternating layers of two materials and represent thus a structure periodic in one dimension. In analogy with lattice planes in a natural crystal, regularly displaced interfaces reflect electromagnetic waves which undergo interference effects. Meaningful reflectivity is obtained at the angles of incidence not far above the critical angle for total reflection. Design flexibility in terms of materials choice and layer thicknesses down to several nm enables us to cover a broad wavelength range from hard X-rays up to deep ultraviolet region where natural crystals are ineffective. Compositionally sharp and geometrically smooth interfaces are required

[1] Presented at SSSI-IV (Solid State Surfaces and Interfaces IV) Conference, Smolenice, Slovakia, 8–11 Nov. 2004.

[2] E-mail address: fyzijerm@savba.sk

0323-0465/05 © Institute of Physics, SAS, Bratislava, Slovakia

for high reflectivity. The interface quality is crucial especially for ultrashort periods approaching 2 nm or less when the layer thicknesses become comparable with the interface widths. After deposition, the interfaces may further degrade due to thermal load at operation. In addition to optical criteria, thermodynamic ones are thus important for the material pair choice. Particularly, interdiffusion, new phase formation, growth mode of one material on the other one and adhesion to the substrate have to be considered.

The work is devoted to Cu/Si and Ni/C multilayer mirrors. They are applicable above 80 keV where W- and Pt- based mirrors exhibit a strong absorption (e.g. gamma telescopes in astronomy) and below the respective metal K edge (around 8 keV — e.g. for Göbel mirrors in diffraction optics). Ni/C mirrors are of interest also for soft X-ray microscopy in the "water window" region between carbon and oxygen K absorption edges (284–543 eV) where the absorption coefficient of water is low. The mirrors work in grazing incidence or normal incidence geometry for hard and soft X-rays, respectively. To minimize optical aberrations, there is always effort to maximize the angle of incidence (measured from the surface) which leads to ultrashort periods.

Long-term room-temperature (RT) stability and narrow interfaces were found in dc sputtered Cu/Si multilayers with the period down to 2 nm [1]. Ni/C multilayers have been studied more frequently. They were prepared mainly by sputtering [2–5] or by pulsed laser deposition (PLD) [6–8]. Sputtered Ni/C mirrors, which were thermally stable up to 300°C, were reported [9, 10]. The interface width proved to be generally larger than in Cu/Si mirrors due to the island growth of Ni. The ultra-high vacuum (UHV) electron beam evaporation was tried only in a few cases [11, 12]. Ion-beam etching of Ni layers was applied to suppress the interface roughness. Comparing with the two other techniques, a lower intermixing and/or interdiffusion at the interfaces may be expected in evaporated multilayers due to less energetic adatoms.

In our work, we test preparation of Cu/Si and Ni/C multilayers by UHV electron beam evaporation with *in situ* substrate heating as a simpler and cheaper alternative to the ion-beam etching. A prolonged surface diffusion length of adatoms induced by the substrate heating is expected to heal the growth related interface roughness. A detailed interface analysis is performed. The work is completed by thermal stability studies to determine the operation temperature limits.

2 Experimental

The multilayers were deposited in UMS 500 Balzers evaporator in the vacuum of 10^{-7} Pa onto silicon wafers with a native oxide layer. The multilayers contained typically 10–15 periods (basic bilayers) of 1.5–3.2 nm. The deposition started with Si (Ni) and the same layer was used as a cover layer. The deposition at various elevated temperatures up to 160°C was applied to optimize the layer growth. A vacuum furnace annealing (10^{-4} Pa) was used to examine the thermal stability.

The multilayer stack was analyzed by the specular X-ray reflectivity (XRR) and X-ray diffuse scattering at grazing incidence (GIXDS). The measurements were performed on a high-resolution diffractometer equipped with a GaAs double crystal monochromator located in the primary beam and providing $CuK_{\alpha1}$ radiation at the output. The divergence and detector slits of 100 μm and 150 μm, respectively, were used. A maximum counting rate of $10^5 s^{-1}$ was within the linear response of a NaI(Tl) scintillation detector. The internal layer structure was examined by X-ray diffraction (XRD) on a Bragg-Brentano powder diffractometer equipped with a

focusing graphite monochromator in the diffracted beam.

3 Results and Discussion

The specular XRR measurements were evaluated by the optical recursive approach [13] supposing error function interface profiles. The specular part of the GIXDS was not included, being by 1-2 orders of magnitude lower than the specular XRR (coherent scattering approximation). The XRR provided the layer thicknesses t and densities ρ as well as the total interface width (effective interface roughness) σ_{eff}. The σ_{eff} value includes all the interface imperfections (roughness, interdiffusion, intermixing) as the scattering vector is normal to the interfaces in an XRR scan. The t and ρ values entered simulations of the GIXDS which is produced solely by geometrical interface roughness. This scattering process was described within the distorted-wave Born approximation (DWBA) [14]. Randomly rough interfaces were supposed which are typical for amorphous and polycrystalline layers found also in our samples by the XRD. Therefore the interface morphology was described within the concept of correlation functions. A lateral correlation function [15]

$$C(r) = \sigma^2 \exp\left[-\left(\frac{r}{\xi}\right)^{2H}\right] \tag{1}$$

was taken the same for all interfaces. Here, σ, ξ, H are the real (geometrical) interface roughness, lateral correlation length and Hurst parameter, respectively, the last one being connected with the fractal interface dimension as D=3-H. The vertical correlation (conformality) of the interface profiles was included by a phenomenological attenuation function with a single vertical correlation length L_{vert}

$$C(z) = \exp\left(-\frac{z}{L_{\text{vert}}}\right) \tag{2}$$

which was convenient in the interval of the roughness frequencies covered by our GIXDS measurements. Several sample and detector scans were measured and then simulated simultaneously for a given sample.

The Cu/Si multilayers were amorphous. Examples of the XRR and GIXDS simulations are shown in Fig. 1 with the simulation parameters indicated in Table 1. An optimized deposition temperature of 80°C provided a minimum interface roughness and extent of intermixing judged from the $\sigma_{\text{eff}} - \sigma$ difference. The reflectivity on the first Bragg maximum approaches 43 percent of the maximum theoretical value which demonstrates a detrimental effect of even a small interface roughness. An asymmetry between the Si-on-Cu and Cu-on-Si interfaces shows that Cu layers grow rougher. The interface widths are rather independent of the multilayer period down to 2 nm and increase below, probably due to agglomeration effects leading to discontinuities in Cu layers which affects both types of interfaces. The vertical correlation length is comparable with the total multilayer thickness giving thus rise to a strong diffuse background around the Bragg peaks. This so-called resonant diffuse scattering is due to constructive interferences of the waves reflected from conformal interfaces. It is a nuisance for imaging application as it lowers the specular contrast.

Tab. 1. The XRR and GIXDS simulation parameters of Cu/Si multilayers. Here, t,Λ, $\sigma_{\rm eff}$, σ, ξ, $L_{\rm vert}$, H stand for the layer thickness, multilayer period, interface width, interface roughness, lateral and vertical correlation lenghts, and Hurst parameter, respectively. Bulk densities of 8.96 gcm^{-3} and 2.33 gcm^{-3} for Cu and Si, respectively, were used for the simulations. The multilayers presented in column 2 and 3 have different nominal periods.

deposition temperature	RT	80°C	80°C
$t_{\rm Cu}$ (nm)	1.22	1.27	0.65
$t_{\rm Si}$ (nm)	2.25	1.9	0.98
Λ (nm)	3.47	3.17	1.63
$\sigma_{\rm eff\ Si-on-Cu}$ (nm)	0.7	0.5	0.7
$\sigma_{\rm eff\ Cu-on-Si}$ (nm)	0.6	0.45	0.6
$\sigma_{\rm Si-on-Cu}$ (nm)	0.4	0.3	—
$\sigma_{\rm Cu-on-Si}$ (nm)	0.35	0.25	—
ξ (nm)	10	10	—
$L_{\rm vert}$ (nm)	30	30	—
H	0.2	0.3	—

A quickly saturating reflectivity drop at RT by $\approx$ 25 percent was observed after deposition of Cu/Si multilayers. A similar effect was reported for sputtered Cu/Si mirrors [1]. A 100°C/1h

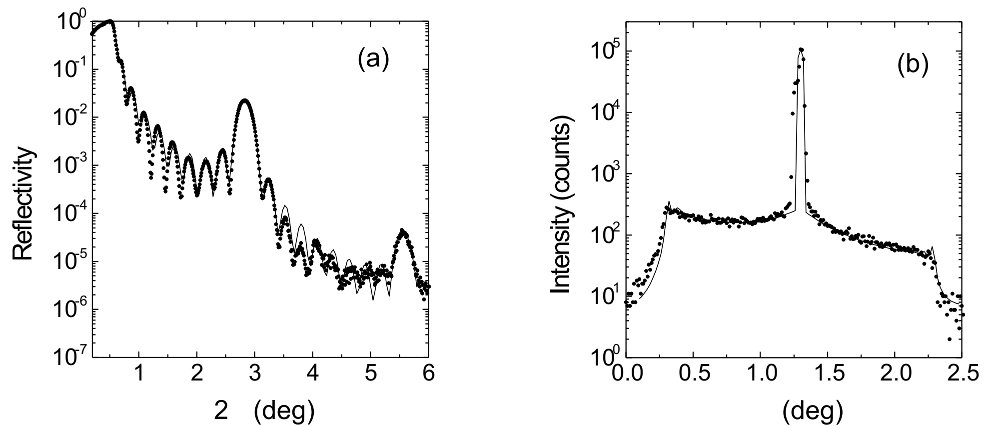

Fig. 1. The specular XRR (a) and GIXDS (b) curves for a Cu/Si multilayer deposited at 80°C with the simulation parameters indicated in Table 1. The latter curve was measured by a sample scan with the detector fixed at the first Bragg maximum. 2θ and ω are the angles between the primary and reflected beams and the angle of incidence, respectively (dots — measured points, line — simulation).

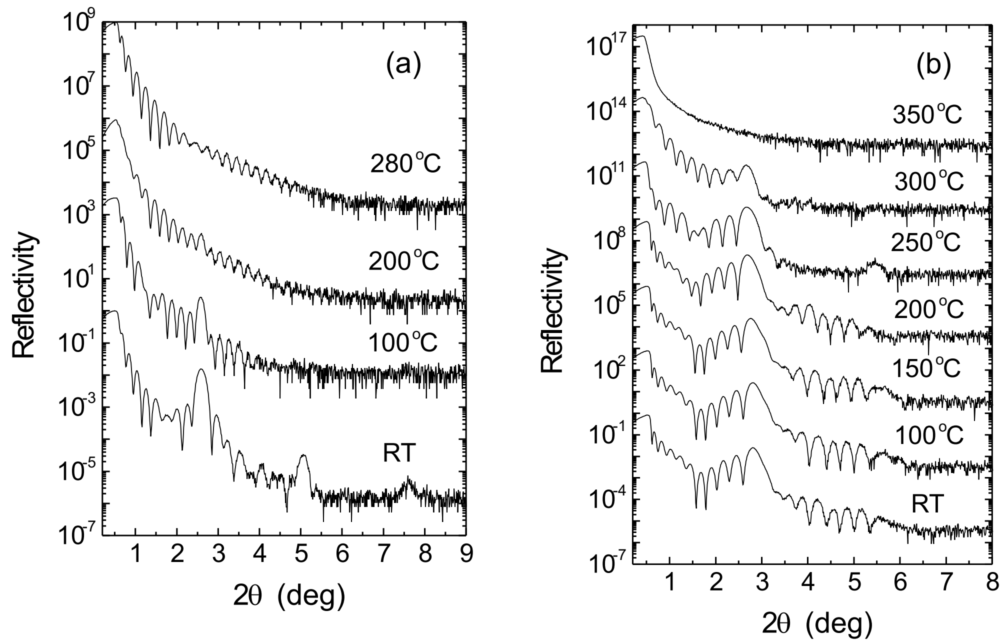

Fig. 2. Thermal evolution of the XRR of a Cu/Si multilayer deposited at RT presented in Table 1 (a) and Ni/C multilayer presented in Table 2 (b). Different pieces from the same Cu/Si multilayer were annealed for 1 hour at the temperatures indicated while one piece of the Ni/C multilayer was exposed to a cumulative annealing for 4 hours at each temperature indicated. The curves are gradually shifted upwards for the sake of clarity.

vacuum annealing brought about a severe suppression of the Bragg peaks (Fig. 2) which disappeared completely on the 200°C/1h one. Contrarily, Kiessig fringes were still preserved even on the 280°C/1h treatment. These results indicate a strong mixing and diffusion at the interfaces leading to the multilayer breakdown while the interface with the substrate is still not smeared completely. An onset of η' (Cu,Si) tetragonal phase formation at 2θ = 44.02° and 58.94° (JCPD-ICDD data set file no. 23-0224), presumably in the intermixed regions, was observed in the diffraction pattern on the 200°C/1h annealing. Fast grain- boundary diffusion of silicon into copper then accelerates the multilayer degradation. Silicon is the main diffuser in the copper-silicon couple.

The interface quality is more sensitive to the deposition temperature in Ni/C multilayers where only close to 80°C it was possible to obtain a well resolved Bragg peak in the XRR curve (Fig. 3). The simulation parameters (Table 2) show the interface widths close to those achieved in Ni/C multilayers deposited by sputtering [2] or UHV evaporation with in situ ion etching [11]. A comparison with the Cu/Si multilayer of a similar period grown at 80°C (Table 1) indicates a larger interface asymmetry which is mainly due to larger extent of the intermixing and interface

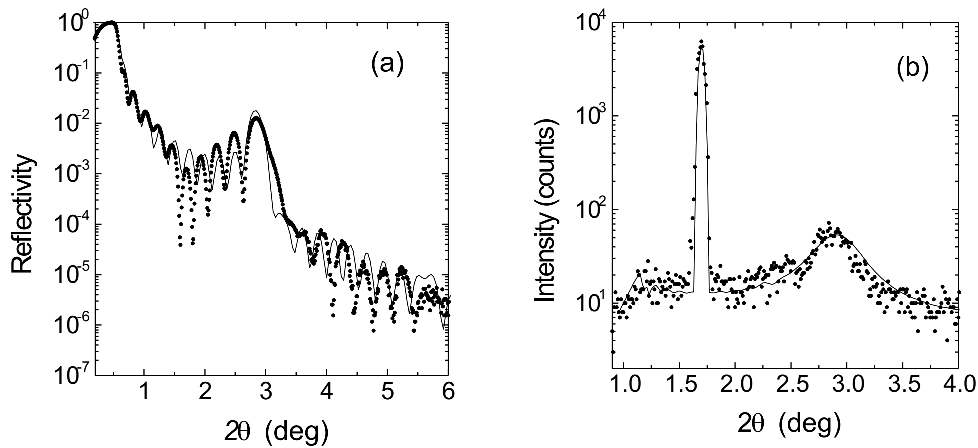

Fig. 3. The specular XRR (a) and GIXDS (b) curves for a Ni/C multilayer deposited at 80°C with the simulation parameters indicated in Table 2. The latter curve was measured by a detector scan with the detector fixed at the first Bragg maximum (dots — measured points, line — simulation).

roughness of the C-on-Ni interfaces. While the intermixing is due to the diffusion of carbon into nickel during the deposition, the larger roughness is induced by the Ni layer growth. We observed the interface widths increasing to 1 nm when the multilayer period decreased below 3 nm suggesting agglomeration effects in Ni. This finding compares well with a percolation threshold of ≈ 2 nm, at which Ni forms coalescent layers, found in sputtered samples [16]. The interface correlation lengths are much shorter than in Cu/Si multilayers (cf. Table 1 and Table 2) while fractal behaviour ($H < 1$) is observed in all cases. Such a behaviour was reported for Ni/C multilayers previously from atomic force microscopy [5].

A step-like vacuum annealing from 100°C up to 350°C with a 50°C step and lasting 4 hours at each step was applied to the sample presented in Fig. 3. After each annealing, the sample was cooled down in vacuum and measured at RT. A gradual increase of the $\sigma_{\mathrm{eff}} - \sigma$ difference (Table 2) indicates that the interdiffusion proceeds. A decrease of the Ni layer densities in the advanced stages of the annealing shows that the dominant diffuser is carbon. The multilayer breakdown occurs on the 350°C annealing (Fig. 2). Here, even Kiessig fringes are not visible in the XRR curve which indicates a complete disintegration of the bottom Ni layer.

The as-deposited Ni/C multilayers are amorphous as detected by the XRD. There is a systematic decrease of the C layer densities correlated with an increase of the multilayer period starting at 150°C (Fig. 4). A similar period increase, amounting to 12 percent, was reported in sputtered Ni/C multilayers [3, 17] and was explained by a transformation of the amorphous into the graphitic-like structure in carbon layers. We could observe this process by the XRD only in advanced stages due to the small scattering volume and weak scattering power of carbon. The graphitization affects only slightly the interface widths before the carbon diffusion into nickel develops at higher temperatures. Carbide crystallization is dominant after the multilayer col-

Tab. 2. The XRR and GIXDS simulation parameters of a Ni/C multilayer deposited at 80°C. Here, ρ is the layer density; 4 hour annealings at each temperature were successively applied to the same sample.

annealing temperature	as-deposited	100°C	150°C	200°C	250°C	300°C
t_{Ni} (nm)	1.26	1.26	1.28	1.32	1.33	1.34
t_{C} (nm)	1.89	1.89	1.92	1.98	1.99	2.01
Λ (nm)	3.15	3.15	3.2	3.3	3.32	3.35
ρ_{Ni} (g/cm^3)	8.9	8.9	8.9	8.5	8.5	8.0
ρ_{C} (g/cm^3)	2.2	2.2	2.1	2.0	2.0	1.8
$\sigma_{\mathrm{eff\ C-on-Ni}}$ (nm)	0.65	0.65	0.7	0.75	1.1	1.6
$\sigma_{\mathrm{eff\ Ni-on-C}}$ (nm)	0.45	0.45	0.5	0.55	0.7	1.2
$\sigma_{\mathrm{C-on-Ni}}$ (nm)	0.35	—	—	—	0.5	0.8
$\sigma_{\mathrm{Ni-on-C}}$ (nm)	0.25	—	—	—	0.3	0.4
ξ (nm)	5	—	—	—	8	10
L_{vert} (nm)	10	—	—-	—	3	‘1
H	0.25	—	—	—	0.18	0.25

lapses. Crystalline grain growth in very thin layers governs also the interface morphology and is reflected in an increase of the lateral correlation length and decay of the interface conformality.

It is noteworthy that a slight increase of the reflectivity on the first Bragg maximum is observed on the 100°C annealing (Fig. 4). A similar effect on a 100°C annealing was observed also in sputtered Ni/C mirrors which were thermally stable up to 300°C [9, 10]. In PLD deposited mirrors, an improvement of the reflectivity induced by a 300°C annealing was found [7] which was attributed to the spinodal decomposition.

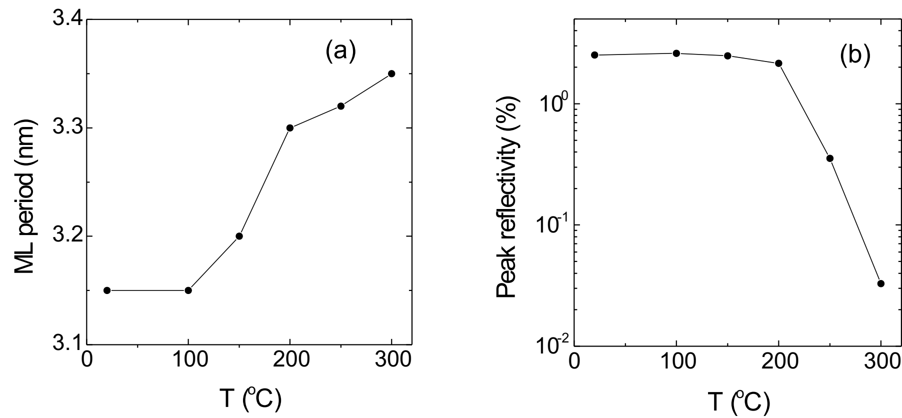

Fig. 4. Temperature evolution of the multilayer period and peak reflectivity on the first Bragg maximum of a Ni/C multilayer annealed as indicated in Table 2.

4 Conclusions

UHV electron-beam evaporation onto a heated substrate proved to be a promising method to prepare ultrashort period Cu/Si and Ni/C mirrors. Their quality and thermal stability is fully comparable with the mirrors of larger periods deposited by other techniques.

A deposition temperature of 80°C provided the best resolved and most intense Bragg peaks in the XRR curve for both types of multilayers. The build-up of the interface roughness, mainly determined by the metal layer growth, is minimized at this deposition temperature while the intermixing between the constituents is not developed yet. As-deposited Ni/C multilayers exhibit a larger roughness and intermixing at the metalloid-on-metal interfaces and are more prone to form discontinuous layers at extremely short periods which are better accessible in Cu/Si mirrors. On the other hand, Ni/C multilayers exhibit the breakdown at a temperature which is by more than 250°C higher than for Cu/Si ones. In fact, Cu/Si multilayers are applicable only at operation temperatures below 100°C because Bragg peaks in the XRR curve were severely reduced on the 100°C/1h annealing. Ni/C multilayers are superior to Cu/Si ones also in terms of smaller correlation lengths resulting in less intense resonant diffuse scattering around the Bragg peaks. This feature has positive implications for specular imaging contrast.

Acknowledgement: This work was partly supported by the Slovak governmental project no. 2003-SO 51/03R0600/01, Slovak grant agencies APVT, project no. APVT-51-021702, and VEGA, project no. 2/3149/23, and COST P7 Action. V. Holý is acknowledged for providing the DWBA software.

References

[1] D.L. Windt: *Appl. Phys. Letters* **74** (1999) 2890
[2] J. Friedrich, I. Diel, C. Kunz, S. Di Fonzo, B.R. Müller, W. Jark: *Appl. Optics* **36** (1997) 6329
[3] V. Dupuis, M.F. Ravet, C. Tete, M. Piecuch, Y. Lepetre, R. Rivoira, E. Ziegler: *J. Appl. Phys.* **68** (1990) 5146
[4] C. Borchers, C. Michaelsen: *Phil. Mag. A* **82** (2002) 1195
[5] M. Ulmeanu, A. Serghei, I.N. Mihailescu, P. Budau, M. Enachescu: *Appl. Surf. Sci.* **165** (2000) 109
[6] N.V. Kovalenko, S.V. Mytnichenko, V.A. Chernov: *JETP Letters* **77** (2003) 80
[7] V.A. Chernov, E.D. Chkalo, N.V. Kovalenko, S.V. Mytnichenko: *Nucl. Instr. & Methods A* **448** (2000) 276
[8] R. Dietsch, T. Holz, T. Weissbach, R. Scholz: *Appl. Surf. Sci.* **197** (2002) 169
[9] G.S. Lodha, S. Pandita, A. Gupta, N.V. Nandedkar, K. Yamashita: *J. Electr. Spec. and Related Phenomena* **80** (1996) 453
[10] K. Nakajima, S. Aoki, S. Sudo, S. Fujiwara: *J. Appl. Phys.* **31** (1992) 2864
[11] Pershin, Y.N. Zubarev, V.V. Kondratenko, O.V. Poltseva, A.G. Ponomarenko, V.A. Servryukova, J. Verhoeven: *Metallofizika i Noveishie Tekhnologii* **24** (2002) 795
[12] E.I. Puik, M.J. Van der Wiel, H. Zeulenmaker, J. Verhoeven: *Appl. Surf. Sci.* **47** (1991) 251
[13] J.H. Underwood, T.W. Barbee: *AIP Conf. Proc.* **75** (1981) 170
[14] V. Holý, T. Baumbach: *Phys. Rev. B* **49** (1994) 10668
[15] S.K. Sinha, E.B. Sirota, S. Garoff, H.B. Stanley: *Phys. Rev. B* **38** (1988) 2297
[16] C. Borchers, P. Ricardo, C. Michaelsen: *Phil. Mag. A* **80** (2000) 1669
[17] T. Djavanbakht, V. Carrier, J.M. Andre, R. Barchewitz, P. Troussel: *J. de Physique IV* **10** (2000) 281